Geophys. J. R. astr. Soc. (1986) **84**, 139–152

Geomagnetic field analysis – IV. Testing the frozen-flux hypothesis

Jeremy Bloxham and David Gubbins *Bullard Laboratories, University of Cambridge, Madingley Road, Cambridge CB3 0EZ*

Accepted 1985 June 4. Received 1985 May 21; in original form 1985 March 18

Summary. We present a model of the magnetic field at the core–mantle boundary, for epoch 1959.5, based on a large set of observatory and survey measurements. Formal error estimates for the radial field at the core are 50 μT, compared with 30 and 40 μT for our previous *MAGSAT* (1980) and *POGO* (1970) models.

Current work on the determination of the velocity of the core fluid relies on the assumption that the core behaves as a perfect conductor, so that the field lines remain frozen to the fluid at the core surface. This frozen-flux condition requires that the integrated flux over patches of the core surface bounded by contours of zero radial field remain constant in time. A new method is presented for constructing core fields that satisfy these frozen-flux constraints. The constraints are non-linear when applied to main field data, unlike the case of secular variation which was considered in an earlier paper. The method is applied to datasets from epochs 1969.5 and 1959.5 to produce fields with the same flux integrals as the 1980 model.

The frozen-flux hypothesis is tested by comparing the changes in the flux integrals between 1980/1969.5, 1969.5/1959.5 and 1980/1959.5 with their errors. We find that the hypothesis can be rejected with 95 per cent confidence. The main evidence for flux diffusion is in the South Atlantic region, where a new null flux curve appears between 1960 and 1970, and continues to grow at a rapid rate from 1970 to 1980. However, the statistical result depends critically on our error estimates for the field at the core surface, which are difficult to assess with any certainty; indeed, doubling the error estimates negates the statistical argument. The conclusion is therefore, at this stage, tentative, and requires further evidence, either from older data, if good enough, or from future satellite measurements.

Key words: Earth's core, frozen-flux, geomagnetism, *MAGSAT*, secular variation

1 Introduction

This is the fourth of a series of papers on the analysis of geomagnetic data for models of the magnetic field at the core–mantle boundary. The models are designed to be used for studies

of the dynamics of the core. The first three papers in the series (Gubbins 1983, 1984; Gubbins & Bloxham 1985) will be referred to as papers I, II and III. Papers I and II dealt with secular variation models based on magnetic observatory data; paper III and the present paper are concerned with models of the main field from satellite and survey data.

A knowledge of the magnetic field at the core–mantle boundary, and particularly its rate of change with time, will enable us to investigate the motion of the core fluid and the governing dynamics. There are two ways to approach the problem. One is to use maps of the core field to provide some insight into the processes involved and to construct dynamical models that account for the observations. The other is to use the field lines as tracers for the flow – a purely kinematic approach.

Roberts & Scott (1965) proposed that the core fluid would act as a perfect conductor and the field lines would be frozen into the fluid at the surface of the core, by Alfvén's theorem, and would therefore act as tracers to the flow. The Roberts & Scott hypothesis was developed further by Backus (1968). Among Backus' results is a set of necessary conditions that the radial component of the core field must satisfy to be consistent with the hypothesis. Those lines and points on the core surface where the radial field vanishes, the null-flux lines and points, are material lines and are therefore permanent features: they cannot merge or split or disappear. Furthermore the total flux through a patch on the core–mantle boundary bounded by a null flux curve must remain constant. There are some nine such patches on the core surface today. These conditions can be written as

$$F_i = \int_{S_i} B_r \, dS = \text{constant} \tag{1}$$

where S_i denotes the area of the ith patch.

The splitting of a null flux curve into two curves is not a strong constraint because only a very small amount of dissipation would be required to complete the break. The same remark applies to the merging of two curves. However (1) represents much stronger constraints, which can be tested more readily against data, because it is easier to calculate estimates of averages, such as the integrals in (1), than of point values, such as those required in fixing the locations of the null-flux curves.

In this paper we present field models for three epochs: 1959.5, 1969.5 and 1980.0. We examine the hypothesis that the field has been frozen into the core fluid throughout this 20 yr time span. Satellites and the very large number of aeromagnetic survey measurements made in recent times ensure that these three field models will be much superior to those of any earlier epoch.

There are two ways to test consistency of the data with the frozen-flux constraints (1). One is to compute the flux integrals and compare differences between epochs with the formal error estimates. The other is to construct field models that are entirely consistent with the constraints and to examine the ensuing impairment of fit to the observations. If the increase in the misfit to the data is unacceptably high then the hypothesis must be rejected.

These two methods are entirely equivalent, and the hypothesis tests give identical answers. It is worth calculating the constrained models, however, because they can be used to study the misfit of individual observations and thereby isolate those measurements that are critical in testing the frozen-flux hypothesis. They are also an essential preliminary stage in calculating core velocities, a calculation which is impossible to carry out precisely with field models that are inconsistent with the frozen-flux hypothesis.

In paper II a method was given for calculating models of secular variation that were consistent with the frozen-flux hypothesis. The constraints on secular variation, equivalent

to (1), are linear provided the main field is assumed known. The constraints on the magnetic field are non-linear because the area of integration depends upon the location of the null-flux curve, which in turn depends upon the field. The non-linearity of the constraints demands a somewhat different approach to that used in paper II. The new method is described in the next section.

2 Method

The methods for analysing magnetic field without constraints, and secular variation with constraints, are described in full in papers III and II respectively. Here we describe only the novel aspects of applying frozen-flux constraints to main field data.

Consider the rate of change with time of the magnetic flux through an arbitrary patch of the core–mantle boundary, S. We have

$$\frac{d}{dt}\int_S B_r\, dS = \int_S \frac{\partial B_r}{\partial t}\, dS + \int_{\partial S} B_r \frac{\nabla B_r \cdot \mathbf{u}}{|\nabla B_r|}\, dl$$

which, if S is a null-flux curve, becomes

$$\frac{d}{dt}\int_S B_r\, dS = \int_S \frac{\partial B_r}{\partial t}\, dS.$$

The flux constraints (1) are therefore equivalent to the conditions on secular variation used in paper II.

The constants in (1) are determined by a reference field model $\mathbf{m}_0$. Any other field model, $\mathbf{m}$, must then satisfy

$$\mathbf{F}(\mathbf{m}) = \mathbf{F}(\mathbf{m}_0) = \mathbf{F}_0.$$

We seek models satisfying these constraints. The equations are non-linear in the components of $\mathbf{m}$ and an iterative method is used.

Adopting the notation of paper II we write

$$\mathbf{F}(\mathbf{m}) = \mathsf{L}^{\mathrm{T}}(\mathbf{m})\mathbf{m}.$$

The rectangular matrix L is a function of $\mathbf{m}$, whereas in paper II it was independent of $\mathbf{m}$. The elements of L are given in terms of integrals of surface harmonics over the patches, by equivalent expressions to those in paper II.

The constraints are readily linearized because $\mathbf{m} \cdot d\mathsf{L}^{\mathrm{T}}/d\mathbf{m} = 0$ for patches bounded by null-flux curves. The linearized form is

$$d\mathbf{F}/d\mathbf{m} = \mathsf{L}^{\mathrm{T}}(\mathbf{m}).$$

The constraints are not applied using the Lagrange multiplier technique of paper II. While this method does yield a solution for the iterate m_{i+1} that satisfies the required condition

$$\mathsf{L}^{\mathrm{T}}(\mathbf{m}_i)\mathbf{m}_{i+1} = \mathbf{F}_0 \tag{2}$$

the sequence $\{\mathbf{m}_i\}$ is found to have very poor convergence. Instead the solution is sought using a penalty method, as described by Luenberger (1973). In paper III we sought as our model $\mathbf{m}$ the minimum of an objective function defined as

$$\Phi(\mathbf{m}) = [\boldsymbol{\gamma} - \mathbf{f}(\mathbf{m})]^{\mathrm{T}}\, \mathsf{C}_{\mathrm{e}}^{-1}\, [\boldsymbol{\gamma} - \mathbf{f}(\mathbf{m})] + \lambda\, \mathbf{m}^{\mathrm{T}} \mathsf{C}_{\mathrm{m}}^{-1} \mathbf{m}.$$

In order to satisfy the flux constraints we add to the objective function an additional

term, a penalty term that 'penalises' departures from the constraints. The penalty term is given by

$$\mu |\mathbf{L}^T(\mathbf{m})\mathbf{m} - \mathbf{F}_0|^2$$

where μ is a scalar parameter chosen to scale the terms in the objective function correctly. μ should be chosen sufficiently large to ensure that condition (2) is satisfied to the desired accuracy, but not so large as to dominate the other terms in the objective function completely. For problems in which the individual components of $\mathbf{F}_0$ differ very widely in magnitude it may be necessary to first rescale the constraint equations.

Penalty methods do not represent an exact application of the constraints in the way that Lagrange multipliers do. However, for non-linear problems the constraints must be applied iteratively, and so exact application is never possible.

Equation (9) of paper II is replaced with

$$\mathbf{m}_{i+1} = \mathbf{m}_i + (\mathbf{A}_i^T \mathbf{C}_e^{-1} \mathbf{A}_i + \lambda \mathbf{C}_m^{-1} + \mu \mathbf{L}_i \mathbf{L}_i^T)^{-1} \left[\left[\mathbf{A}_i^T \mathbf{C}_e^{-1} [\gamma - \mathbf{f}(\mathbf{m})] - \lambda \mathbf{C}_m^{-1} \mathbf{m}_i + \mathbf{L}_i (\mathbf{L}_i^T \mathbf{m}_i - \mathbf{F}_0)\right]\right]$$

where $\mathbf{L}_i = \mathbf{L}(\mathbf{m}_i)$.

In practice one finds the overall step length, from the starting model to the constrained model, to be small. This allows a short-cut to be made in the numerical procedure. The normal equations matrix at the ith iteration, $\mathbf{N}_i$, given by

$$\mathbf{N}_i = (\mathbf{A}_i^T \mathbf{C}_e^{-1} \mathbf{A}_i + \lambda \mathbf{C}_m^{-1} + \mu \mathbf{L}_i \mathbf{L}_i^T)$$

need not be fully updated at each iteration. It is sufficient to approximate it with

$$\mathbf{N}_i = (\mathbf{A}_0^T \mathbf{C}_e^{-1} \mathbf{A}_0 + \lambda \mathbf{C}_m^{-1} + \mu \mathbf{L}_i \mathbf{L}_i^T)$$

where $\mathbf{A}_0$ is based on the starting model $\mathbf{m}_0$.

The right side vector is fully updated at each iteration. It has the form

$$\mathbf{r}_i = \mathbf{A}_i^T \mathbf{C}_e^{-1} [\gamma - \mathbf{f}(\mathbf{m}_i)] - \lambda \mathbf{C}_m^{-1} \mathbf{m}_i + \mu \mathbf{L}_i (\mathbf{L}_i^T \mathbf{m}_i - \mathbf{F}_0).$$

3 Data

Data for epochs 1980.0 and 1969.5 were described in paper III of this series. The 1969.5 dataset has been modified slightly, and the 1959.5 set is completely new. Only the new data are discussed here; the reader is referred to paper III for a more complete description of the *MAGSAT* satellite data used for 1980.0 and the *POGO* satellite and observatory data used for 1969.5.

The additional data for epoch 1969.5 are repeat stations from the Australian region. Readings for both 1980 and 1970 were supplied to us by the geomagnetism section of the Bureau of Mineral Resources in Canberra. Twenty of these stations yielded measurements of X, Y and Z at 1970 and 1980 with no site change, for which crustal corrections were calculated by subtracting our core field model for 1980.0 (model D80111 of paper III) from the 1980 observations. These crustal corrections were subtracted from the 1970 readings. A further 58 repeat stations were used without crustal corrections; measurements of X, Y and Z were available in all cases.

Those repeat stations for which a crustal correction was available were assigned an error of 50 nT. This value is slightly larger than the errors assigned to the observatories, reflecting the presumed poorer quality of the repeat station measurements. The residuals for the observatory data for the model D69111 of paper III suggested the assigned errors were too small. The errors were therefore increased for the new calculation by raising the nominal

uncertainty in the crustal corrections from 20 to 30 nT. The errors for observatories and repeat stations with no crustal corrections were reduced from 300 to 200 nT.

It is well known that total intensity data, such as that provided by the *POGO* satellites, yields poor information for the vertical field near the equator (Lowes 1975; Stern & Bredekamp 1975; paper III). The vector data from the Australian repeat stations were added in the hope of providing better resolution of the interesting wave-like feature in the magnetic equator beneath Indonesia. In fact neither the new data nor the different weights produced significant changes in the core field, showing that it was already well determined.

The field model for 1959.5 was based on observatory annual means and survey data from 1954.5 to 1964.5. There are a great deal of survey data from this time because of the efforts made during the International Geophysical Year (IGY). No satellite data were used.

Observatory data were selected and corrections for crustal magnetization applied using the method described in paper III, a simplified version of the method of Langel, Estes & Mead (1982). Many observatories ran continuously from 1959 to 1980. The annual means were plotted for this interval and the plots inspected for any apparent baseline shifts. Any known changes in baseline were applied to the earlier measurements. In some cases further corrections were applied to produce a continuous curve. Observatory records that began up to three years after the 1959.5 date were extrapolated back to the required year. This procedure yielded measurements of X, Y and Z, with crustal corrections, at 119 observatories.

Further observatories were used with crustal corrections calculated from the 1969.5 annual mean and the core field model D69111. The new crustal corrections are listed in Table 1. For 20 observatories the corrections are completely new: the records do not allow a

Table 1

Observatories with anomalies based on 1969.5, no 1980 values available

AG	Agincourt	-91	173	-149
BI	Binza	-85	-126	-115
IB	Ibadan	93	-384	47
KS	Ksara	-69	65	-156
LR	Lwiro	213	62	23
LS	Lisbon	83	15	39
MA	Manhay	-7	-2	199
MC	Moca	-75	-9	259
ML	Misallat	-70	49	107
PA	Paramaribo	-6	20	7
PR	Pruhonice	-56	26	-77
SP	South Pole	-86	5	190
SR	Srednikan	13	9	161
STO	Stonyhurst	-13	10	-104
SW	Swider	-332	-99	230
TI	Tiksi	-115	-149	-114
TM	Tomsk	-49	-68	-255
TP	Teheran	-167	35	-165
TT	Tatuoca	53	-139	139
TW	Trelew	133	27	7
WK	Wilkes	656	-257	80
YS	Syowa Base	-27	-34	7

Observatories with 1980 anomaly that was unreliable and replaced with 1969.5 value

AN	Annamalainaga	230	-92	-66
CQ	Cha Pa	-58	-103	-105
DI	Dikson	-120	-132	-279
SM	San Miguel	683	410	1714
TN	Tananarive	332	-17	-428
TR	Tromso	35	-400	167
VO	Vostok	32	128	155

correction to be based on the 1980.0 core field. For a further seven observatories the 1969.5 corrections were deemed more reliable and used in place of the original 1980.0 corrections, usually because an extrapolation had been used in calculating the latter. The new crustal corrections are listed in Table 1; the three columns are for X, Y and Z respectively.

In all cases an error was assigned to the annual mean which consisted of a 30 nT component, representing the uncertainty in the crustal correction, and a component assessed from the scatter in the plot of data from 1959.5 to 1980.0 and any baseline shifts and extrapolations that had been made.

A further 51 observatories were used without crustal corrections. All but three of these ran for short periods at about the time of the IGY. The remaining three will be useful in deriving core field models for earlier epochs with crustal corrections based on the 1959.5 core fields. These observatories were assigned an error of 200 nT.

The remaining data were taken from two 'Main Field' tapes supplied by World Digital Data Centre C1 at the British Geological Survey in Edinburgh. These tapes contain observations made from 1900 onwards.

A great many repeat stations measurements are available for around 1960. These sites were occupied for a short time, and some attempt would have been made to remove the effects of external currents from the readings. In fact only a minority of these 'repeat' stations have ever been repeated: for example the British sites have never been re-occupied.

Some stations had been repeated for a sufficiently long period of time for a crustal correction to be applied. The 138 stations in this category had been re-occupied at least three times, the first and last times being within three years of 1959.5 and 1969.5 respectively. A straight line was fitted to observations made after 1955.5 and values at the two epochs interpolated from it. The 1959.5 interpolates were corrected for crustal magnetization and weighted in the same way as the corrected observatories.

A further 365 repeat stations were re-occupied with a sufficiently long interval for a correction to be made for secular variation. All stations gave measurements of all three components (X, Y, Z). Most of these stations were in North America, Australia and South Africa. Data from Japan and Europe were not used because these regions are well served by permanent observatories.

The remaining repeat stations yielded 1150 measurements. These were treated in the same way as other survey data. They were corrected for secular variation to epoch 1959.5 and assigned an error of 300 nT. The secular variation and main field models used for the reduction to epoch and starting model for the calculations were supplied by Dr R. A. Langel (Langel *et al.* 1986). They depend upon a spline fit of the time variation of geomagnetic coefficients throughout the twentieth century. The coefficients themselves are derived primarily from observatory annual mean data.

The observatory and repeat station data were augmented by three component marine and project MAGNET data. Most of the 8108 marine measurements were of H, D and Z, made by the Russian survey ship *Zarya*. Although the *Zarya* usually made measurements of four different components of the magnetic field, only three can be used for our procedure. The 'errors' in these measurements are dominated by the crustal magnetization and therefore the 'error' in a fourth component would be dependent on the 'errors' in the first three. The method of analysis relies on independence of the errors, and inclusion of correlated errors would be a serious mistake. The marine data were assigned errors of 300 nT for H and Z; $300/H$ rad for declination, and for inclination $300/F$ rad; total field data were assigned an error of $\sqrt{2} \times 300$ nT. A discussion of errors is given in Barraclough & Malin (1971).

The Project MAGNET data were used to fill in gaps in the data coverage. The MAGNET data are very dense along tracks and only measurements from every fifth point were

retained. It is essential to have a spacing that is larger than the wavelength of the crustal anomalies, otherwise errors in measurements at nearby locations would be correlated. In total 13 357 project MAGNET measurements of F, I and D were used. Errors were assigned using the same scheme as for the marine data, but based on 200 nT rather than 300 nT. The short-wavelength crustal anomalies are attenuated at altitude, and airborne surveys are less affected by them.

This large dataset gave adequate global coverage everywhere except in eastern parts of the Soviet Union, where there was no MAGNET coverage and very few land measurements. This gap was filled with measurements read, at intervals of 4° in latitude and 6° in longitude, from a 1:2 500 000 magnetic chart of total intensity for epoch 1964 edited by M. A. Vasil'eva of the USSR Ministry of Geology. The resulting 152 measurements were assigned errors of $\sqrt{2} \times 300$ nT, as for the marine data.

The complete dataset comprised 24 858 measurements, substantially greater than was used in our models for 1980.0 or 1969.5. However these ground-based and airborne measurements are greatly disturbed by the crustal magnetization, and the overall weight given to the survey data will not be as great as the satellite observations used for later epochs. The crustal corrections applied to the observatories and some repeat stations ensure that our models will include good secular variation information.

4 Results

4.1 MODEL FOR 1959.5

The dataset for 1959.5 was inverted with the dissipation norm and a damping constant of 1.7×10^{-12}, which gave a norm of 135×10^{12}. This choice gave a model with a very similar norm to those at the other two epochs. The misfit was close to unity for all the different types of data, showing the weighting scheme to be satisfactory. Models were also calculated for several other values of the damping constant to provide a trade-off curve. Point estimates for the radial field at the core–mantle boundary were calculated as described in paper III giving a range of 50–58 μT of which 32 μT was the remainder error. This compares with errors of about 28 and 36 μT for the 1980.0 and 1969.5 models. The radial field at the core–mantle boundary for this model is plotted in Fig. 1.

4.2 FLUX FITTING

Using the method described in the previous section, models were produced for epochs 1959.5 and 1969.5 constrained to have the same flux integrals as the reference 1980.0 model (model D80111 of paper III). This model has nine patches; they are plotted in Fig. 2. The patches have been named according to their geographical distribution. An appropriate value of the penalty parameter was found to be 10^{-9}; the procedure converged to within less than 1 MWB for all patches within four iterations. The constrained model for 1959.5 is plotted in Fig. 3. The constrained model for 1969.5 is little different from the corresponding unconstrained model and is not plotted.

The effect of incorporating the flux constraints is to increase the norm. The constraints are satisfied by adding additional high wavenumber terms to the model, so increasing the norm while leaving the misfit little changed. By appropriate adjustment of the damping parameter it would be possible to produce flux-constrained models having similar norm to the unconstrained models, but increased misfit. An estimate of the increase in the misfit can be made using the trade-off curve for the unconstrained model; for 1969.5 it is 0.16 per cent and for 1959.5 it is 0.12 per cent.

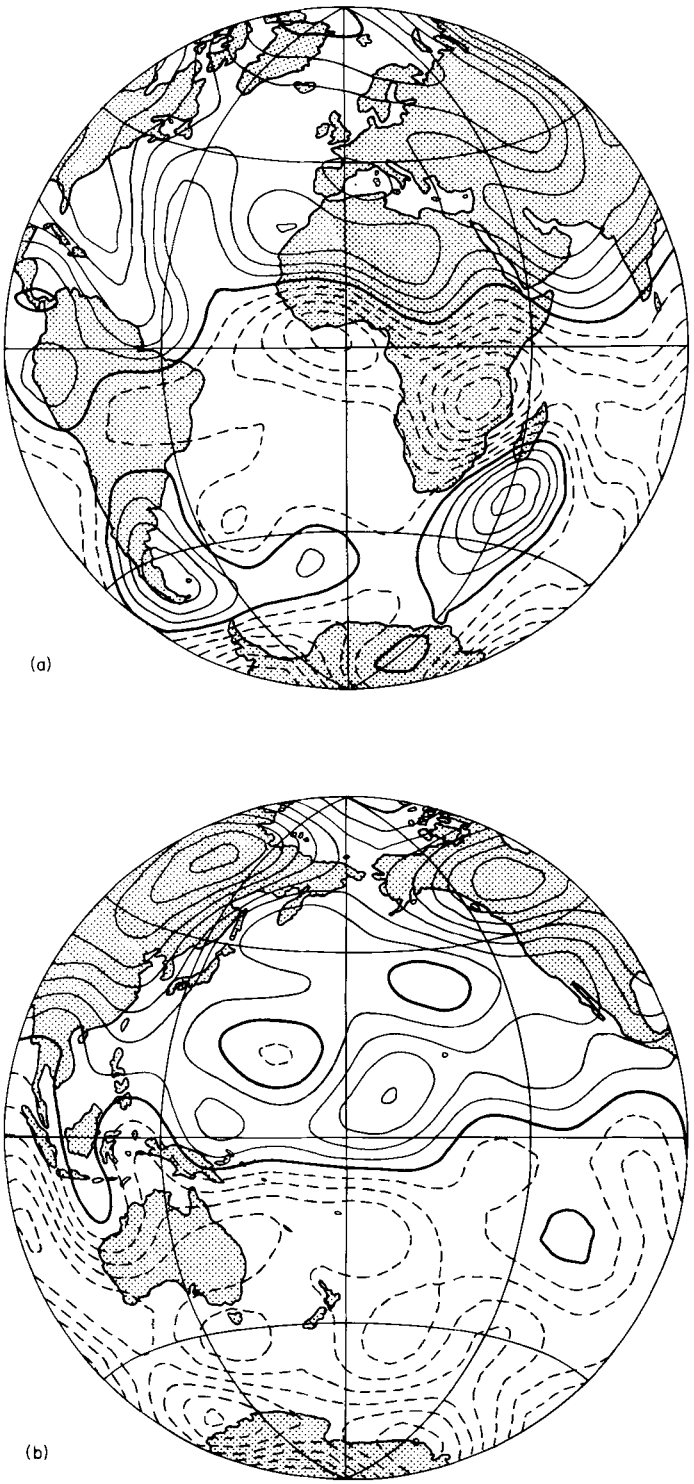

Figure 1. Contours of radial magnetic field at the core–mantle boundary for epoch 1959.5. Dashed contours are positive, thick lines are zero contours, and the contour interval is 100 μT.

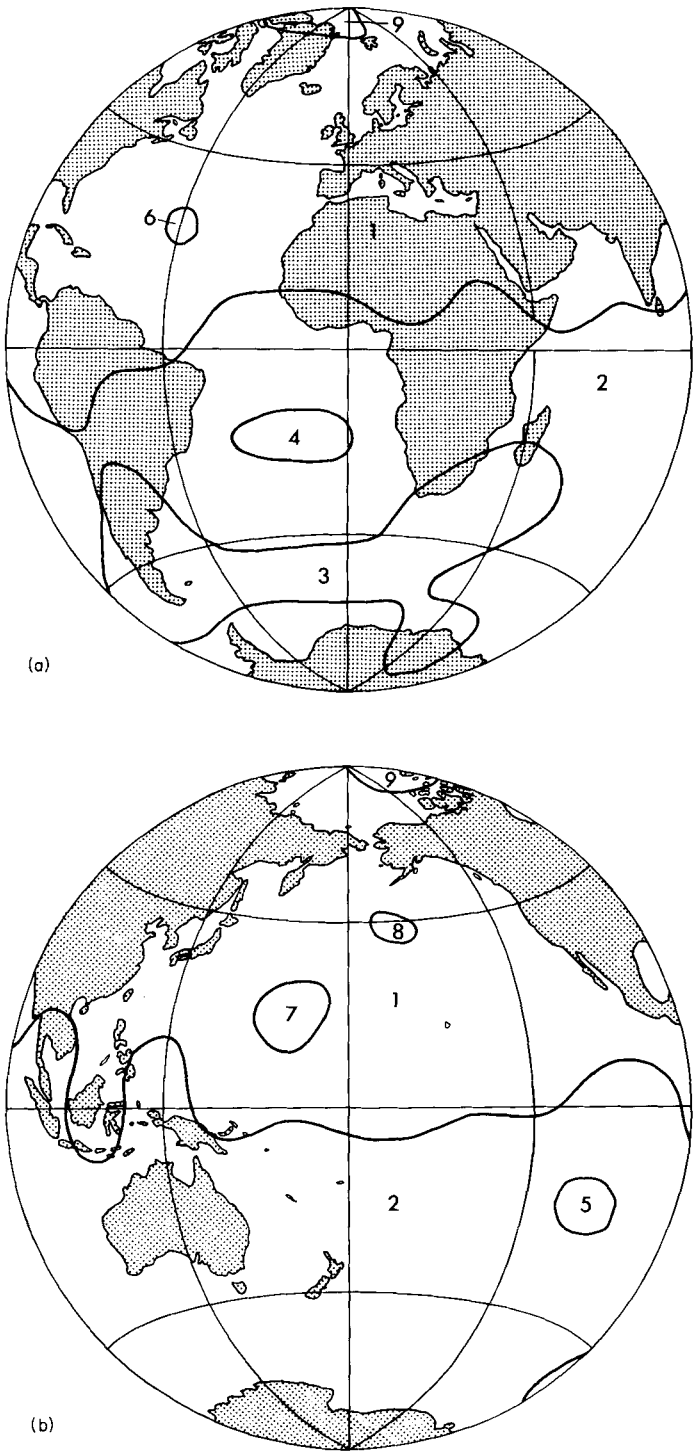

Figure 2. Null-flux curves for the model D80111, epoch 1980.0. The numbers correspond to the names in Table 2. This model was used to define the flux integrals used in calculating the fields for epochs 1969.5 and 1959.5 that are consistent with frozen flux.

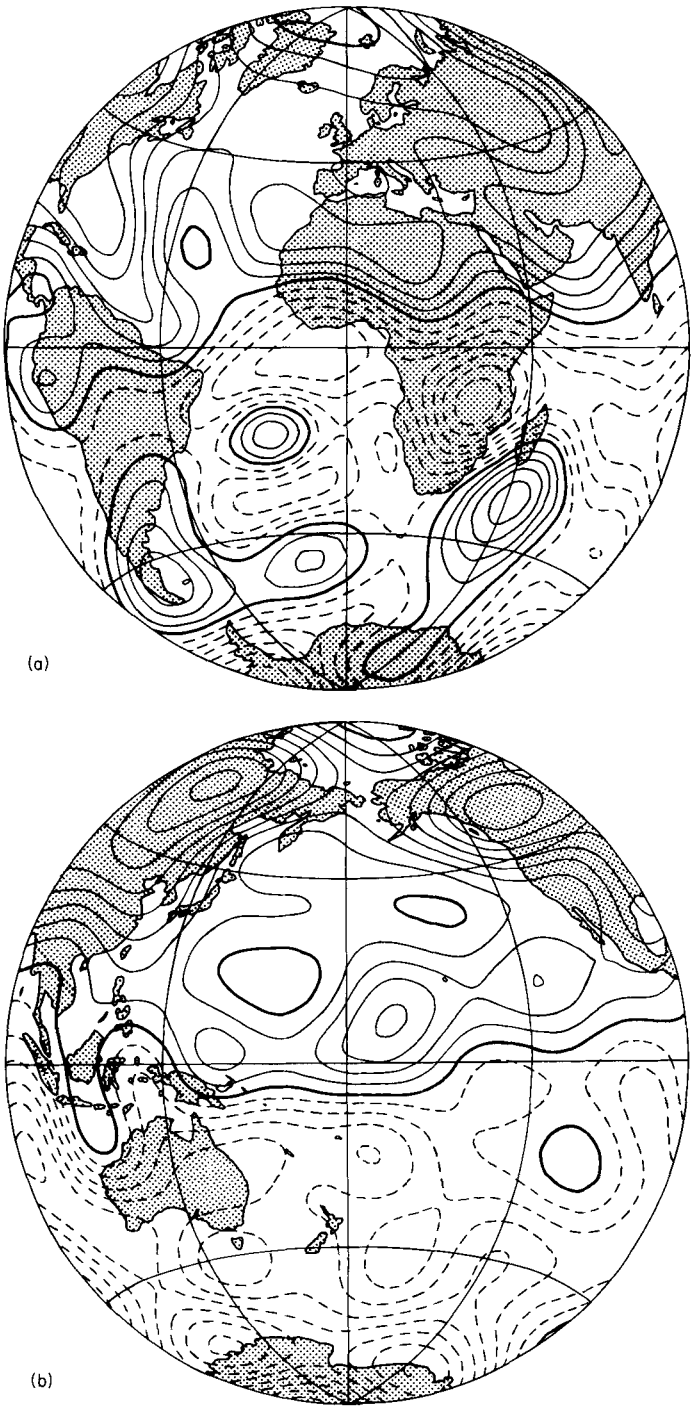

Figure 3. Contours of radial field for epoch 1959.5. This field has the same flux integrals as model D80111 for epoch 1980.0. The three null-flux curves in the far South Atlantic region have been treated as one, equivalent to contour 3 in Fig. 2. This map is to be compared with that of the unconstrained model in Fig. 1. Although many features of the maps are similar, the constrained model has an extra null-flux curve (number 4).

4.3 ERROR ANALYSIS OF THE FLUX INTEGRALS

In order to test the frozen-flux hypothesis we need to calculate the values of the flux integrals and assess whether they are constant in time. This demands error bars to be placed on the estimates of the integrals. Our procedure gives a covariance matrix for the geomagnetic coefficients up to spherical harmonic degree and order 20, and it is straightforward to compute the contribution to the variance of the integrals. The contribution from higher-order terms must also be estimated because it will not, in general, be negligible. The error analysis was described in paper I, where the special case of integrals over the geographic northern hemisphere was discussed. Here we consider more general patches.

The remainder variance is the contribution to the variance of an integral from terms of degree higher than 20. It is given by the expression

$$V_R = \sum_{l>20} V_l \left[\left(\frac{a}{c}\right)^{l+2} (l+1) \int_{S_i} Y_l^m \, dS\right]^2$$

where V_l is the variance of coefficients of degree l and the Y_l^m are Schmidt quasi-normalized spherical harmonics. In order to estimate v_R we assume l to be large and take a typical value of Y_l^m to be $0(l^{1/2})$. Since Y_l^m is an oscillating function with at least l zeros on the sphere, their integrals will, provided the patch is sufficiently large to enclose several zeros, obey the approximate inequality

$$\int_{S_i} Y_L^m \, dS \leqslant \frac{4\pi c^2}{l^{3/2}}$$

leading to, with the choice of v_l used for these models,

$$V_R \leqslant \sum_{l>20} \frac{1}{4\pi\lambda} \left(\frac{a}{c}\right)^4 \frac{(2l+1)^2}{l^7} (4\pi c^2)^2 .$$

The calculated terms show the asymptotic regime is reached by degree 15. The dependence on l is observed to be close to l^{-6}, indicating the estimate to be pessimistic. It is adequate for our purposes, however. We write

$$V_R \leqslant \sum_{l>20} \frac{k}{l^5} \cong \frac{k}{4(20)^4}$$

and estimate k from the calculated term in the sum for $l = 20$. Taking the South Atlantic null-flux curve as an example we find $k = 1.4 \times 10^{19}$ for model D80111 and hence $v_R < 2 \times 10^{13}\,\mathrm{Wb}^2$. This corresponds to an error of $5 \times 10^6\,\mathrm{Wb}$ which is an order of magnitude less than the contribution from terms of degree 20 and below, and may therefore be neglected.

5 Conclusions

In this section we seek to determine whether the data are consistent with the frozen-flux hypothesis. Table 2 shows the changes in the flux integrals for the periods 1980.0/1969.5, 1969.5/1959.5 and 1980.0/1959.5, together with errors for these changes.

We wish to test the null hypothesis H : $\mathbf{L}^T\mathbf{m} = \mathbf{F}_0$. We assume that the constraints may be linearized with sufficient accuracy; words of caution similar to those used in paper II, for the interpretation of the errors in the radial field, are attached to the interpretation of the

Table 2. Flux integrals (MWb).

	Patch	1980.0	1969.5	1959.5	80-70	Error	70-60	Error	80-60	Error
1	Northern Hemisphere	-17547	-17469	-17533	-78	45	64	77	-14	74
2	Southern Hemisphere	18850	18691	18590	160	51	100	88	260	84
3	South Atlantic	-1274	-1250	-1115	-25	32	-104	56	-129	54
4	St. Helena *	-88	-50	*	-38	15	(-50)		(-88)	
5	Easter Island	-20	-41	-10	21	14	-31	23	-10	21
6	North Atlantic	3	5	0	-2	7	5	8	3	4
7	North West Pacific	2	10	21	-8	9	-11	21	-19	20
8	North East Pacific	33	35	61	-2	14	-25	27	-27	27
9	North Pole	39	66	15	-27	15	50	20	23	19

* this flux patch absent from 1959.5 field model

statistical inferences to be made here. We require further that the matrix L is of full rank: one constraint must be dropped. We choose the North Atlantic patch.

Searle (1971) shows that the statistic: $\mathfrak{F} = Q\hat{\sigma}^2/N_c$ has F-distribution:

$$F_{N_c,N_F}(\lambda)$$

where

$$Q = (\mathsf{L}^T\mathbf{m} - \mathbf{F}_0)^T (\mathsf{L}^T \mathsf{G} \mathsf{L})^{-1} (\mathsf{L}^T\mathbf{m} - \mathbf{F}_0)$$

$$G = (\mathsf{A}^T \mathsf{C}_e^{-1} \mathsf{A} + \lambda \mathsf{C}_m^{-1})^{-1}.$$

N_c is the number of constraints retained, N_F is the number of degrees of freedom in the unconstrained model, $\lambda = Q/2\hat{\sigma}^2$ is the non-centrality parameter of the distribution. Under the null hypothesis, λ is zero. As the number of data are large, we have

$$\mathfrak{F} \approx F_{N_c,\infty}.$$

Now from paper II we have the model covariance matrix given by

$$\mathsf{C} = \hat{\sigma}^2 (\mathsf{A}^T \mathsf{C}_e^{-1} \mathsf{A} + \lambda \mathsf{C}_m^{-1})^{-1}$$

so

$$\mathfrak{F} = (\mathsf{L}^T\mathbf{m} - \mathbf{F}_0)^T (\mathsf{L}^T \mathsf{C} \mathsf{L})^{-1} (\mathsf{L}^T\mathbf{m} - \mathbf{F}_0)/N_c.$$

$\mathfrak{F}$ is the mean square weighted residual to the constraints.

Testing the hypothesis for the interval 1980.0/1969.5 we find that $\mathfrak{F} = 3.27$ from which we reject the frozen-flux hypothesis with greater than 99.5 per cent confidence.

Testing the hypothesis over the intervals 1969.5/1959.5 and 1980.0/1959.5 presents a dilemma: the St Helena patch is absent from the 1959.5 field model and so cannot be directly included in the calculation of the statistic $\mathfrak{F}$. However, the very absence of this patch in 1959.5 represents very strong evidence in favour of rejection of the hypothesis.

Calculating $\mathfrak{F}$ for the remaining patches we find

$\mathfrak{F} = 2.09$ for 1969.5/1959.5,

$\mathfrak{F} = 2.70$ for 1980.0/1959.6,

representing rejection at greater than 95 and 99 per cent confidence respectively.

Alternatively we may include the St Helena patch as a part of the South Atlantic patch and calculate their contribution as one composite patch. We then find

$\mathfrak{F}$ = 2.68 for 1969.5/1959.5,

$\mathfrak{F}$ = 4.23 for 1980.0/1959.5,

representing rejection with greater than 99 and 99.5 per cent confidence respectively. An alternative statistical test might be proposed based on the degradation in misfit to the data resulting from applying the conditions as equality constraints. However, as Searle (1971) shows, such a test would be formally equivalent to the test already considered; indeed the quantity Q is sufficient to calculate the resultant degradation in misfit.

The constrained model is useful, though, for checking the compatibility of the various categories of data (e.g. marine survey, repeat stations) with the hypothesis. It is conceivable that rejection of the hypothesis may result from, for example, errors in the project MAGNET data in the South Atlantic Ocean, perhaps because of an error in the baseline of the data; a consistent error of 250 nT, over a large number of observations, could account for the absence of this null-flux curve. Comparison of the degradation in misfit to the various categories of data was examined in order to attempt to detect such an effect.

The residuals to the constrained model were compared with those of an unconstrained solution (with the same value of the norm) for the various categories of data for 1959.5. Although no compelling evidence was found for such an effect, the absence of the St Helena null-flux patch is not established beyond all doubt. Additional models of the field, which are currently in preparation, for epochs both close to 1959.5 and earlier than 1959.5, should enable us to determine the behaviour of the field in this region with more confidence.

It is worthwhile to note that the rejection of the null-flux hypothesis is largely the result of changes taking place in the field under the southern half of the Atlantic Ocean. A substantial proportion of these changes can be accounted for by the emergence of new field lines from the core from the St Helena and South Atlantic patches which re-enter the core through the Southern Hemisphere patch.

The tentative conclusion of this analysis must be to reject the frozen-flux hypothesis, even on the time-scale of just a decade. The confidence levels of over 99 per cent are certainly high but depend critically upon our error estimates. The errors need only to be doubled in order to remove almost all evidence against the frozen-flux hypothesis. We must seek further evidence for changes in the flux integrals, either from models pre-dating 1960 or from future satellite data.

Acknowledgments

We thank D. R. Barraclough and D. Kerridge of the British Geological Survey in Edinburgh and A. J. McEwin of the Bureau of Mineral Resources in Canberra for supplying data and for their advice, and R. C. Bailey for helpful discussions. JB is supported by a NERC studentship. This work is supported by NERC grant GR3/3475.

References

Backus, G. E., 1968. Kinematics of geomagnetic secular variation in a perfectly conducting core, *Phil. Trans. R. Soc. A*, **263**, 239–266.

Barraclough, D. R. & Malin, S. R. C., 1971. Synthesis of international geomagnetic reference field values, *NERC Inst. geol. Sci. Rep. No. 71/1*.

Gubbins, D., 1983. Geomagnetic field analysis – I. Stochastic inversion, *Geophys. J. R. astr. Soc.*, **73**, 641–652.

Gubbins, D., 1984. Geomagnetic field analysis – II. Secular variation consistent with a perfectly conducting core, *Geophys. J. R. astr. Soc.*, **77**, 753–766.

Gubbins, D. & Bloxham, J., 1985. Geomagnetic field analysis – III. Magnetic fields on the core mantle boundary, *Geophys. J. R. astr. Soc.*, **80**, 696–713.

Langel, R. A., Estes, R. H. & Mead, G. D., 1982. Some new methods in geomagnetic field modelling applied to the 1960–1980 epoch, *J. Geomagn. Geoelect.*, **34**, 327–349.

Langel, R. A., Kerridge, D. J., Barraclough, D. R. & Malin, S. R. C., 1986. Geomagnetic temporal changes: 1903–1982, A spline representation, in preparation.

Lowes, F. J., 1975. Vector errors in spherical harmonic analysis of scalar data, *Geophys. J. R. astr. Soc.*, **42**, 637–651.

Luenberger, D. G., 1973. *Introduction to Linear and Nonlinear Programming*, Addison-Wesley, Reading.

Roberts, P. H. & Scott, S., 1965. On analysis of the secular variation I. A hydromagnetic constraint, *J. Geomagn. Geoelect.*, **17**, 137–151.

Searle, S. R., 1971. *Linear Models*, Wiley, New York.

Stern, D. P. & Bredekamp, J. H., 1975. Error enhancement in geomagnetic models derived from scalar data, *J. geophys. Res.*, **80**, 1776–1782.